Journal of Physiology (1993), **466**, *pp.* 501–520
With 9 figures
Printed in Great Britain

LOSS OF Na^+ CHANNEL INACTIVATION BY ANEMONE TOXIN (ATX II) MIMICS THE MYOTONIC STATE IN HYPERKALAEMIC PERIODIC PARALYSIS

BY STEPHEN C. CANNON* AND DAVID P. COREY*†

*From the *Department of Neurology, Howard Hughes Medical Institute, Massachusetts General Hospital, Boston, MA 02114, USA and the † Program in Neuroscience, Harvard Medical School, Boston, MA 02114, USA*

(*Received 6 August 1992*)

SUMMARY

1. Mutations that impair inactivation of the sodium channel in skeletal muscle have recently been postulated to cause several heritable forms of myotonia in man. A peptide toxin from *Anemonia sulcata* (ATX II) selectively disrupts the inactivation mechanism of sodium channels in a way that mimics these mutations. We applied ATX II to rat skeletal muscle to test the hypothesis that myotonia is inducible by altered sodium channel function.

2. Single-channel sodium currents were measured in blebs of surface membrane that arose from the mechanically disrupted fibres. ATX II impaired inactivation as demonstrated by persistent reopenings of sodium channels at strongly depolarized test potentials. A channel failed to inactivate, however, in only a small proportion of the depolarizing steps. With micromolar amounts of ATX II, the ensemble average open probability at the steady state was 0·01–0·02.

3. Ten micromolar ATX II slowed the relaxation of tension after a single twitch by an order of magnitude. Delayed relaxation is the *in vitro* analogue of the stiffness experienced by patients with myotonia. However, peak twitch force was not affected within the range of 0–10 μM ATX II.

4. Intracellular injection of a long-duration, constant current pulse elicited a train of action potentials in ATX II-treated fibres. After-depolarizations and repetitive firing often persisted beyond the duration of the stimulus. Trains of action potentials varied spontaneously in amplitude and firing frequency in a similar way to the electromyogram of a myotonic muscle. Both the after-depolarization and the post-stimulus firing were abolished by detubulating the fibres with glycerol.

5. We conclude that a loss of sodium channel inactivation alone, without changes in resting membrane conductance, is sufficient to produce the electrical and mechanical features of myotonia. Furthermore, in support of previous studies on myotonic muscle from patients, this model provides direct evidence that only a small proportion of sodium channels needs to function abnormally to cause myotonia.

INTRODUCTION

The myotonias constitute a group of heritable muscle disorders that share a common phenotype of delayed relaxation of tension after contraction and enhanced electrical excitability of the muscle membrane (for review, see Rüdel & Lehmann-Horn, 1985). The latter is manifest by trains of repetitive discharges that arise from the muscle independent of neural input and that may occur either spontaneously, after voluntary contraction, or following direct muscle percussion. Various physiological bases for the altered electrical excitability in myotonic muscle have been proposed for several disorders and model systems.

A reduced chloride conductance has been firmly established as one cause of myotonia. Bryant (1962) first showed that muscle from myotonic goats has an abnormally high membrane resistance due to a pronounced reduction of the chloride conductance. He also demonstrated that normal muscle develops myotonia when placed in chloride-free saline. Adrian & Bryant (1974) later concluded that an accumulation of potassium in the T-tubule is also required to drive the train of action potentials that outlasts the duration of the stimulus. A low chloride conductance is the cause of both a dominant (Thomsen's Disease) and recessive (Becker-type) form of congenital myotonia in man (Lipicky, Bryant & Salmon, 1971; Koch *et al.* 1992) and of a recessive form of myotonia in mice (Mehrke, Brinkmeir & Jockusch, 1988; Steinmeyer *et al.* 1991).

A persistent or non-inactivating inward sodium current has also been proposed to cause myotonia in both disease and model systems. Hyperkalaemic periodic paralysis (HPP) is a dominantly inherited disorder characterized by episodic attacks of transient weakness, induced by elevated serum potassium. In many families myotonia occurs around the time of an attack. Lehmann-Horn, Küther, Ricker, Grafe, Ballanyi & Rüdel (1987) and Ricker, Camacho, Grafe, Lehmann-Horn & Rüdel (1989) demonstrated a tetrodotoxin-sensitive, persistent inward current in muscle removed by biopsy from patients with HPP. They concluded that a non-inactivating sodium current depolarizes the muscle and thereby produces paralysis. Cannon, Brown & Corey (1991) showed that the functional defect in the sodium channels of HPP muscle is a failure to inactivate when the extracellular potassium is elevated. The proportion of mutant channels that resides in the non-inactivating mode at any one time is small, however: only 5–10 % with 10 mM extracellular [K^+]. The activation and unitary conductance of the mutant channels are normal. Linkage between the gene coding for the adult muscle isoform of the sodium channel α-subunit on chromosome 17q, SCN4A, and the expression of symptoms has been established for both HPP (Fontaine *et al.* 1990) and another disorder, paramyotonia congenita (Ebers *et al.* 1991; Ptacek *et al.* 1991*b*). Two different mutations have been identified in SCN4A in families with HPP (Rojas, Wang, Schwartz, Hoffman, Powell & Brown, 1991; Ptacek *et al.* 1991*a*). Either mutation alone is proposed to be sufficient to cause the phenotype. For paramyotonia congenita, two different point mutations have been identified in SCN4A as well (McClatchey *et al.* 1992). All the mutations identified are transversions of a single base, which results in the substitution of a single, highly

conserved, amino acid residue. Either HPP mutation introduced into the rat skeletal muscle α-subunit cDNA will cause sodium channel dysfunction characteristic of human HPP myotubes (Cannon & Strittmatter, 1993). The primary objective of the present study was to verify that the small proportion of non-inactivating sodium channels we previously identified in myotubes cultured from patients with HPP is sufficient to produce myotonia.

Exogenous agents that potentiate sodium currents can produce a myotonic state in normal muscle. Most widely known are veratridine and related alkaloid toxins which induce spontaneous twitching and trains of action potentials in nerve and muscle preparations, even in the presence of curare (Ulbricht, 1969). These agents not only impede inactivation of sodium channels at depolarized potentials, but also shift the voltage dependence of activation by 90 mV in the negative direction (Leibowitz, Sutro & Hille, 1986). Consequently veratridine-modified sodium channels are not a good model of the defect in HPP. A better tool is a polypeptide toxin isolated from *Anemonia sulcata*, ATX II, which binds to an external site of the sodium channel and decreases the rate of inactivation without affecting activation (Bergman, Dubois, Rojas & Rathmeyer, 1976). Across different species and tissues, nerve and muscle preparations possess varying degrees of sensitivity and reversibility to the effects of ATX II. Tesseraux and co-workers have demonstrated that ATX II increases force, lengthens the duration of action potentials, and may produce repetitive firing in a variety of mammalian muscle preparations (Alsen, Harris & Tesseraux, 1981; Harris, Pollard & Tesseraux, 1985).

We have reinvestigated the effects of ATX II on mammalian skeletal muscle as a model for the sodium channel defect in HPP. In particular, we show that the threshold concentration of ATX II required to produce a myotonic twitch response is 10 μM, and that this concentration causes a steady-state open probability of 0·02 as determined by single channel measurements. Thus the small proportion of non-inactivating sodium channels recorded in HPP muscle with elevated external [K^+] (Cannon *et al.* 1991) is probably sufficient to cause myotonia.

METHODS

Muscle preparation

The extensor digitorum longus (EDL) was dissected from Long–Evans rats that had been anaesthetized with a lethal dose of pentobarbitone, 50 mg intraperitoneally. All rats were females which were approximately 1 week postpartum, having been purchased with litters for other experiments. The full-length muscle, from tendon to tendon, was placed in a mammalian saline solution (Table 1), gassed with 95 % O_2–5 % CO_2, and kept at room temperature (22–24 °C). Toxin purified from *Anemonia sulcata* (ATX II, Sigma, St Louis, MO, USA) was frozen in 2 ml aliquots at a concentration of 10 μM in saline solution. Varying concentrations of ATX II were prepared by diluting freshly thawed stock solution with saline.

Single channel recordings

Unitary sodium currents were recorded from spheres of sarcolemmal membrane that were mechanically disrupted from small bundles of muscle fibres. Cell-free membrane spheres were produced by a modification of the method described by Stein & Palade (1989). In mammalian saline solution, a bundle of 2–5 fibres, 1–2 cm long, was dissected away from the tendon. The bundle was then cut from the remainder of the muscle and transferred to the recording chamber which was filled with the Cs^+ bath solution described in Table 1. The free ends of the bundle were grasped with fine forceps, and the fibres were stretched to 3–4 times the rest length with a

succession of three or four rapid movements. The bundle was then released and allowed to settle to the bottom of the chamber. Over 15–30 min, blebs of sarcolemmal membrane, 10–50 μm in diameter, spontaneously pinched off the fibres and settled on the floor of the chamber. Patch electrodes could then be gently pressed against these spheres to form tight seals (> 50 GΩ) and

TABLE 1. Composition of solutions (mM)

Mechanical response and action potentials

	K^+	Na^+	Ca^{2+}	Mg^{2+}	Cl^-	$H_2PO_4^-$	HCO_3^-	Dextrose
Saline*	4·5	146	2	1	130·5	1	25	12

Single channel recording

	Cs^+	Na^+	Ca^{2+}	Cd^{2+}	$CH_3SO_3^-$	Cl^-	Dextrose	Hepes
Bath	145	0	2	0	145	4	5	5
Electrode	0	140	2	0·1	140	4·2	5	5

* Gassed with 95 % O_2–5 % CO_2, pH 7·3–7·4, and 10 μg/l curare added.

sodium currents were recorded in the 'bleb-attached' configuration. Inside-out patches could be pulled from the membrane spheres, but they were mechanically less stable than bleb-attached ones. The spheres were not sturdy enough to break the membrane patch with suction to switch to a 'whole-bleb' configuration or to obtain outside-out patches.

Patch electrodes were fabricated from 1·5 mm borosilicate capillary tubing (Kwik-fill, WPI Sarasota, FL, USA) with a two-stage puller. The electrode was then coated with Sylgard to reduce capacitance and fire polished for a final tip internal diameter of 0·5 μm, corresponding to a DC resistance of 10 MΩ. Electrode and bath solutions listed in Table 1 were chosen to isolate Na^+ currents by blocking Ca^{2+} and K^+ currents, and by reducing the available Cl^-. The voltage dependence of sodium channel gating indicated that the transmembrane potential for the bleb-attached patches was approximately zero.

Single channel currents were measured with a Dagan 3900A patch-clamp amplifier using a capacitance-coupled headstage. The amplifier output was filtered at 2 kHz (4-pole Bessel) and sampled at 10 kHz with the LM900 Laboratory Interface (Dagan, Minneapolis, MN, USA) controlled by a 486-based computer (Northgate, Minneapolis, MN, USA). Voltage command potentials were generated by the computer. For bleb-attached patches, the electrode tip was held 120 mV from bath ground and stepped to varying test depolarizations as indicated in figure legends. Capacitance transients were determined from the average of twenty-five small amplitude depolarizations for which no channels opened. This leak trace was then scaled and subtracted on-line from the current evoked during a test depolarization.

Twitch force measurements

The EDL was stretched to approximately 1·3 times the slack length during twitch measurements of isometric twitch force. One end was pinned to the bottom of a Sylgard-coated Petri dish. The other tendon was tied to a force transducer with suture material. The transducer was constructed from a piezoelectric bimorph element that produces a potential difference when mechanically deformed. The device was light and stiff, with a natural frequency greater than 1 kHz and a linear output over the calibration range of up to 270 mN. The transducer output was low-pass filtered at 500 or 200 Hz and digitized at 10 or 1 kHz, respectively. The muscle was stimulated directly by passing current between two chlorided silver wires placed along the entire length of the muscle. A stimulus isolation unit was gated with 5 ms pulses, generated every 20 s under computer control. Current intensity was set at a value twice the threshold required to produce a measurable twitch. *d*-Tubocurarine chloride (Sigma) was added to the bathing solution (10 μg/l) to block neuromuscular transmission.

The twitch response was characterized by the peak force and a relaxation time. For many trials the decrease in force was not a single exponential. Often a plateau occurred after the peak, and during the onset and wash-out of toxin a multi-exponential decay with two dominant time constants was observed. The relaxation of force did, however, always follow a monotonically

decreasing time course. Any monotonically decreasing process, $y(t)$, can be quantitatively characterized by a relaxation time, T_r:

$$T_r = \frac{1}{y(t_0)} \int_{t_0}^{\infty} y(t)\mathrm{d}t.$$

For the special case of an exponential process in which $y(t) = y(t_0)e^{-t/\tau}$ then T_r equals τ, the time constant. When $y(t)$ is not a single exponential, then T_r can be interpreted as a temporal index of the relaxation process: the area under the response curve, normalized by the peak amplitude. It is the time constant for the exponential decay that best approximates the actual data.

Action potential recordings

Action potentials were recorded from surface fibres of the EDL, which was stretched and pinned to the bottom of a Sylgard-coated Petri dish. Curare was added to block neuromuscular transmission. Electromechanical coupling was disrupted with Dantrolene (2–4 mg/l; Sigma) so that action potentials could be measured without motion artifacts (Ellis & Bryant, 1972). Electrodes were pulled from 1·5 mm borosilicate capillary tubes. A voltage-sensing electrode was filled with 3 M KCl. A second electrode was placed 40–80 μm from the first electrode to inject current and contained 2 M potassium citrate. Electrode resistances were 10–20 MΩ. With the use of an agar bridge, the junction potential of the recording electrode was less than 5 mV. A hyperpolarizing holding current was passed to set the resting potential to −90 mV. Depolarizing current steps from 10 to 200 nA were applied by an Axoclamp-2A amplifier in bridge mode (Axon Instruments, Foster City, CA, USA). The second channel of the Axoclamp-2A was used as an electrometer to record the transmembrane voltage. The transmembrane voltage was filtered at 3 kHz and sampled at 10 kHz.

For one set of experiments, fibres were detubulated to decouple electrically the T-tubule from the surface membrane (Dulhunty & Gage, 1973). The whole muscle was immersed in mammalian saline plus 400 mM glycerol for 1 h. Upon returning to normal saline, the muscle twitched spontaneously for up to 30–40 min, even in the presence of Dantrolene. Once the spontaneous mechanical activity had ceased, stable electrical recordings could be obtained without mechanical artifact.

RESULTS

Sodium channel behaviour

The ability of this toxin model to mimic the sodium channel defect identified in muscle from patients with HPP was verified by measuring single channel behaviour in sarcolemmal blebs. The majority of bleb-attached patches contained sodium channels which were recognized by their characteristic voltage dependence of gating. Figure 1*A* shows currents recorded from normal muscle during sixteen consecutive depolarizing steps, presented at an interval of 0·5 s. After a short latency, sodium channels opened transiently (downward deflections) and then entered an inactive state from which further openings did not occur during the remainder of the depolarization. The time-dependent open probability, $P_{open}(t)$, is shown below the individual trials in Fig. 1, and was computed as the ensemble average of 128 trials divided by the number of channels in the patch. The latter was assumed to equal the maximum number of simultaneous openings observed during the entire lifetime of a patch, a period which included at least 1024 test depolarizations. In patches from control fibres, $P_{open}(t)$ increased to a peak between 0·35 and 0·5, and then decreased rapidly and completely to zero within a few milliseconds.

Sodium channels exposed to ATX II displayed markedly abnormal kinetics of inactivation. The extracellular face of sodium channels was exposed to ATX II by adding the toxin to the electrolyte in the recording pipette. Toxin concentrations

greater than 1 μM impeded the formation of gigaohm seals with the membrane spheres. Good seals were achieved for high concentrations of toxin, however, by immersing the tip of the electrode into control electrolyte solution and then backfilling the shank with the toxin solution. Diffusion of toxin down to the tip of

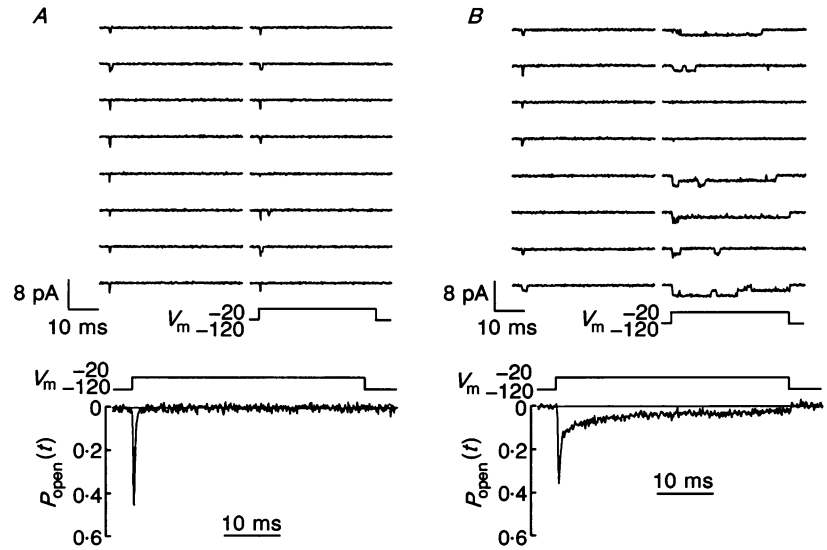

Fig. 1. Sodium channel gating in normal (*A*) and ATX II-exposed patches (*B*). Each panel shows 16 consecutive responses to a 40 ms depolarizing step, recorded from bleb-attached patches. Channel openings produce downward deflections in the current tracings. Capacitance transients have been subtracted. Lower traces show the time course of the open channel probability, computed from the ensemble average of 128 trials. Number of channels per patch was estimated to be two for *A* and three for *B*, based on the maximum number of simultaneous openings observed in over 1024 trials. V_m is the command potential (millivolts) relative to the rest potential.

the electrode reached a steady state within 1 or 2 min of seal formation as evidenced by the dramatic effect of toxin on channel gating. The analysis of channel gating included only sweeps that were recorded after 10 min of patch lifetime. In 10 μM ATX II, sodium channels gated normally for most of the depolarizing steps, as shown in the first eight trials on the left of Fig. 1*B*. For other test depolarizations, however, the inactivation process was severely disrupted. One or more channels entered and left a non-inactivating mode on a slow time scale, which caused traces with non-inactivating behaviour to occur in clusters of consecutive depolarizations (Fig. 1*B*). Channels in the non-inactivating mode had markedly prolonged dwell times in the open state and repetitively opened and closed during the entire depolarization. The loss of inactivation altered $P_{open}(t)$ such that it no longer decayed to zero, even after the entire 40 ms of depolarization.

The time-averaged open probability, measured late in the depolarization, was used as a quantitative index for the loss of sodium channel inactivation. First, raw traces were idealized as the number of open channels at each point in time, using a

50 % unitary current amplitude criterion to discriminate openings. $P_{open}(t)$ was then computed from the ensemble average of the idealized records. The time-averaged open probability, $< P_{open} >$, was defined as the mean value of $P_{open}(t)$ over the interval from 5 to 40 ms. Figure 2 shows the increase in $< P_{open} >$ with

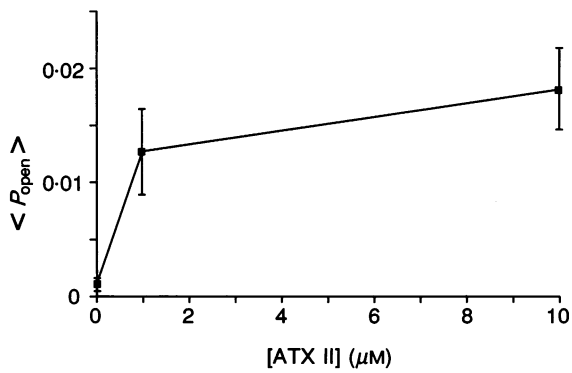

Fig. 2. Probability of a sodium channel persistently residing in the open state due to ATX II. For each patch, $< P_{open} >$ was computed as the temporal average of $P_{open}(t)$ over the interval 5–40 ms. Symbols depict the mean ± S.E.M. computed by combining data from multiple patches (0 μM, $n = 6$; 1 μM, $n = 2$; 10 μM, $n = 5$).

increasing concentrations of ATX II. For depolarizations in the range −40 to −10 mV, $< P_{open} >$ was independent of membrane voltage, and data were pooled for all trials in a given patch. Control patches with no toxin have a non-zero value for $< P_{open} >$ of 0·0011 because brief openings were occasionally observed with latencies greater than 5 ms. In 10 μM ATX II $< P_{open} >$ was 0·018, which implies that in toxin-exposed muscle about 2 % of the total population of sodium channels remained open at any instant during the depolarization.

Other biophysical properties of sodium channel function were not as severely altered by ATX II. Sodium ion conductance was increased, but only mildly. Figure 3 shows unitary current amplitudes measured at varying test potentials in one control and two toxin-exposed patches. The slope conductance was 18·7 pS for the control patch and 20·1 and 21·8 pS with toxin. Linear extrapolation of the control data predicts a reversal potential of 53 mV. The activation of sodium channels was not modified by ATX II. For both toxin-exposed and control patches, sodium channel openings did not occur at hyperpolarized holding potentials (−100 to −90 mV) and were observed frequently only for depolarizations to −50 mV or greater. Because most patches contained more than one sodium channel, it was not possible to perform an accurate estimate of latency to first opening. It was evident, however, that the initial rising phase of $P_{open}(t)$ was not different between control and ATX II-treated patches. Finally the voltage dependence of the maximum in $P_{open}(t)$ was unaffected by ATX II. Thus, ATX II mimics the functional defect in sodium channels from HPP muscle: a persistent current due to a small proportion of non-inactivating channels with no alteration in activation or conductance.

Mechanical responses

Isometric twitch responses were measured from whole muscle that was stretched to 1·3 times the slack length and stimulated by passing current between two longitudinally placed wires. In control muscle, a 5 ms shock elicited a rapid rise in

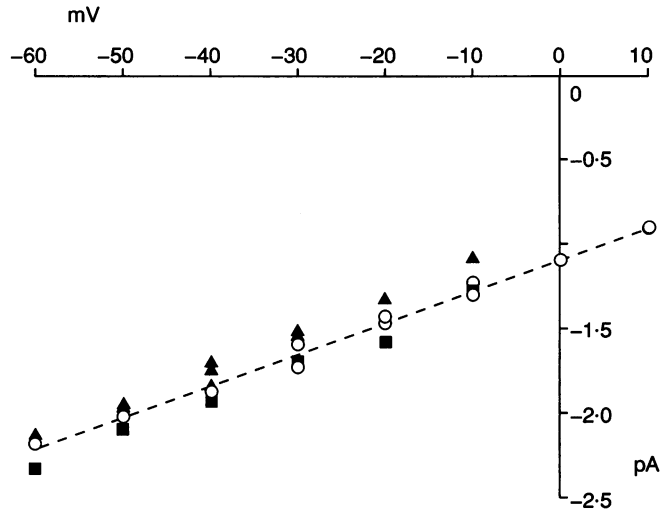

Fig. 3. Single channel current–voltage relationship. All measurements were made from bleb-attached patches. Dashed line is fitted by linear regression analysis to the control patch (○; no ATX II). The other two patches (■, ▲) were exposed to 10 μM ATX II. Holding potential was −120 mV.

tension to about 100 mN followed by a slower monotonic decay to the resting level. After establishing the control response, the bath was exchanged with saline containing toxin and allowed to equilibrate for 15 min. The primary effect of ATX II on the twitch response of the EDL was a marked prolongation of the relaxation phase. The twitch responses at four different bath concentrations of ATX II have been normalized in amplitude and superimposed in Fig. 4*A* to illustrate the effect on the kinetics of the mechanical response. At the highest concentration of toxin, 10 μM, the rise time was slowed moderately while the relaxation was prolonged 17-fold. This abrupt transition between normal and prolonged relaxation occurred between 1 and 10 μM ATX II in all three muscles tested. Figure 4*B* shows a dose–response curve for the relaxation time, defined in the Methods, as a function of toxin concentration. In one preparation, 20 μM ATX II was applied, but did not cause a further increase in the relaxation time. For economic reasons, higher bath concentrations of toxin were not tested. The mean increase in relaxation time in 10 μM ATX II was 13-fold ($n = 3$ muscles). This 'all-or-none' effect was also demonstrated during recovery from the toxin effect as

shown in Fig. 4*D*. The maximal toxin effect was first obtained by bathing the muscle in 10 μM ATX II for 45 min. The recovery was then monitored by measuring the twitch response at varying times after initiating continuous perfusion with saline. The rate of toxin removal is undoubtedly not uniform

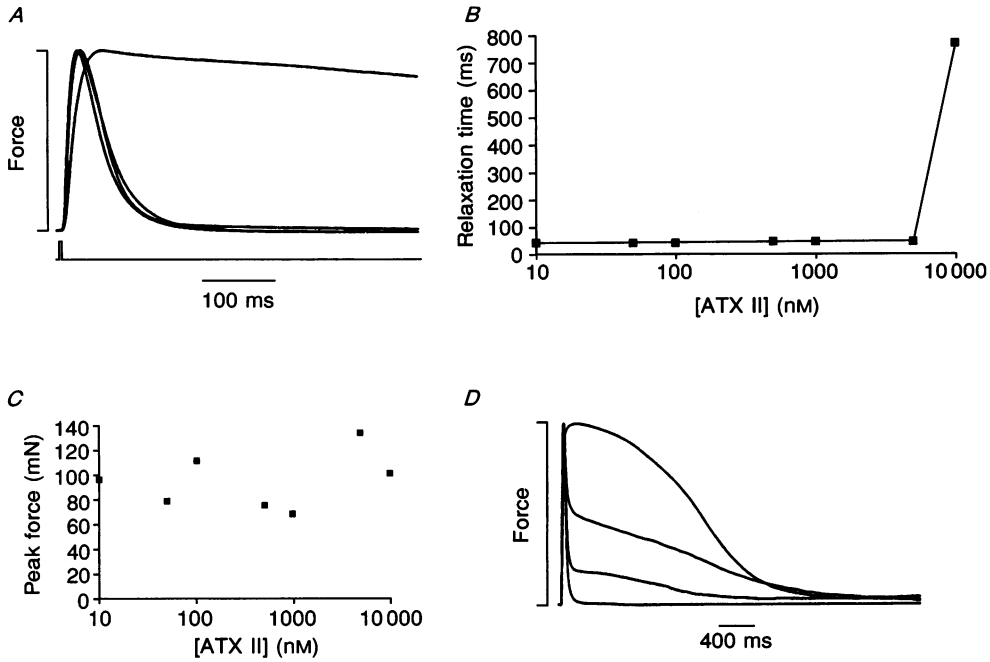

Fig. 4. Twitch response of an ATX II-treated EDL muscle. *A*, superposition of twitch force measured from the same muscle bathed in 0·1, 1, 5 and 10 μM ATX II. Amplitude has been normalized to the peak response. Duration of the electrical stimulus is shown below the force trace. Stimulus intensity was set at twice the threshold for detecting a change in resting tension. *B*, relaxation time and *C*, peak twitch force measured 15 min after exposure to various concentrations of ATX II. *D*, recovery of twitch relaxation recorded after washing for 0, 30, 90 and 150 min. The muscle was previously bathed in 10 μM ATX II for 45 min. All responses in Fig. 4 were recorded from a single muscle preparation. Similar responses were seen in three preparations.

throughout the thickness of this whole muscle preparation due to the substantial barriers to diffusion. In spite of this probable gradation in the local concentration of toxin among individual fibres, the mechanical response consistently produced a weighted sum of two distinct relaxation patterns – normal and markedly prolonged. There was no continuous gradation in relaxation time. Rather, the mechanical response was a superposition of normal and prolonged patterns. Before wash-out, the twitch response was dominated by the prolonged component of the relaxation. With progressively longer washing, the slowly relaxing component of the twitch response diminished in amplitude until the toxin effect was completely reversed.

There was no consistent effect of ATX II on the amplitude of the twitch response. The twitch amplitude at varying concentrations of ATX II is shown in Fig. 4*C*. These responses are from the same experiment as in Fig. 4*B*. Although relaxation was prolonged markedly, the peak force developed during a twitch was

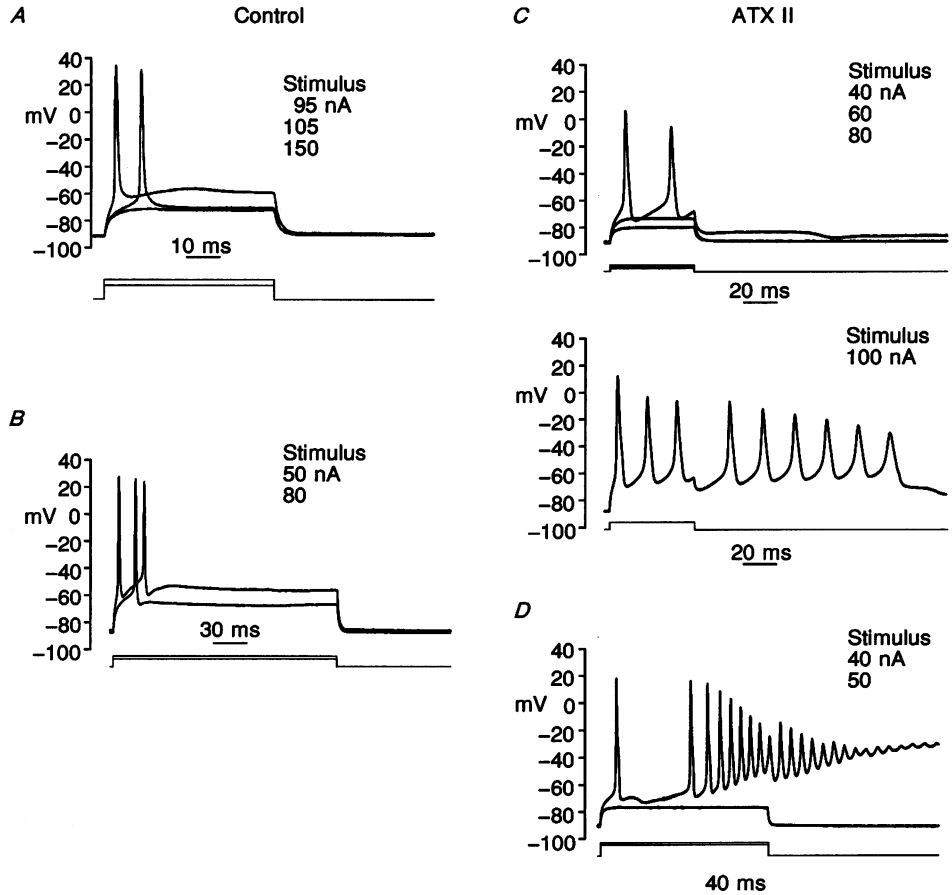

Fig. 5. Action potentials triggered by long-duration current injection in control (*A* and *B*) and ATX II-treated fibres (*C* and *D*). In *A*, three responses are superimposed, which were elicited by currents ranging from subthreshold to 1·5 × threshold intensity. *B*, a control fibre fired a doublet of spikes at 1·25 × threshold current intensity. *C*, a fibre bathed in 10 μM ATX II fired repetitively during current injection. At higher current intensity, spikes persisted after the stimulus ended. *D*, another ATX II-treated fibre demonstrates that runs of action potentials occurred at threshold in some instances.

relatively unaffected. The resting tension between twitches was not monitored for different concentrations of toxin because the transducer was zeroed between measurements. We did, however, observe fasciculations of individual fibres lasting several minutes after the electrical stimulus while the muscle was bathed in 10 μM ATX II. These asynchronous contractions of individual fibres did not produce detectable fluctuations in the force transducer output above the background noise level.

Action potentials in ATX II-treated fibres

Electrical responses were recorded from surface fibres impaled with two microelectrodes. One electrode recorded the transmembrane potential and the second electrode, placed 50–100 μm away, passed the stimulus current. ATX II induced hyperexcitability of the muscle membrane. Micromolar concentrations of toxin (1) caused repetitive firing of action potentials in trains that at times outlasted the duration of the stimulus, (2) increased the duration of the action potential, and (3) created a second possible resting potential which was shifted in the depolarizing direction.

The change in transmembrane potential in response to long-duration, constant-current injection is shown in Fig. 5 for normal and ATX II-treated fibres. Control fibres produced only a single action potential at the threshold current intensity, even when the current injection was maintained long after the action potential. In most fibres, current injections of 1·5–2 times threshold also elicited a single action potential, as shown in Fig. 5*A*. For approximately 25 % of control fibres, suprathreshold stimulations produced two, or at most three action potentials (Fig. 5*B*). In all cases, the fibre stopped firing well before the end of the current injection. Multiple action potentials, when present, tended to occur in fibres for which the Dantrolene treatment was only partially successful in blocking a twitch. This suggests that a mechanical disruption of the membrane may have created an increased leak current that depolarized the cell and elicited multiple spikes.

In 10 μM ATX II all fibres produced trains of multiple action potentials for suprathreshold current injection. For just-threshold stimulation some fibres continued to generate a single spike as shown in Fig. 8*C*, but others produced sustained trains of spikes even at threshold (Fig. 5*D*). The minimum toxin concentration required to produce repetitive firing in the EDL was 50 nM. Concentrations in excess of 100 nM, however, were needed to observe repetitive firing regularly. ATX II-treated fibres often continued to fire action potentials even after the depolarizing current was switched off (Fig. 5*C* and *D*). These after-spikes never occurred in control fibres and were common only for toxin concentrations of 5–10 μM. Whenever these after-spikes occurred, there was a progressive depolarization during the stimulation. This can be seen in Figs 5*D* and 8*A* and *B* as the upward drift in the potential at the end of each action potential. As the single-channel data demonstrated, only a small proportion of sodium channels failed to inactivate in 10 μM ATX II. Consequently, the depolarizing shift inactivated sodium channels that were still functioning normally. The reduction in the number of available sodium channels was manifest as a decrease in the rate of rise and the amplitude of the action potentials.

Three different responses were observed after a train of spikes. The firing sometimes continued after the end of the stimulus, with a progressive depolarizing shift until the cell reached a plateau depolarization of −50 to −40 mV and became refractory to firing (Fig. 5*D*). In other fibres action potentials continued transiently after the stimulus, but at a slower frequency, and eventually stopped as the normal resting potential was re-established (Fig. 5*C*). Or, finally, a depolarized after-potential occurred without superimposed firing (Fig. 8*A*).

The duration of the action potential was prolonged by ATX II. Figure 6 compares the time course of spikes elicited by brief current injections in control and ATX II-treated fibres. Prolongation of the action potential duration was at most 2- to 3-fold at the maximum concentration of ATX II used in these experiments,

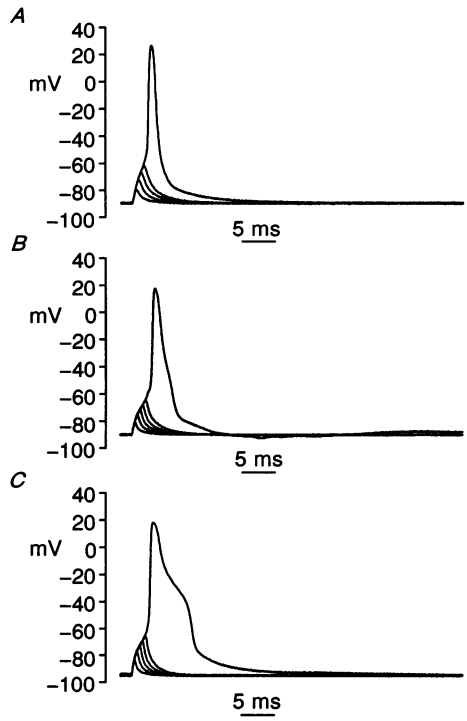

Fig. 6. Prolongation of action potentials by ATX II. Responses to progressively longer duration current injection (200 nA) are shown in controls (*A*, same fibre as shown in Fig. 5*B*) and fibres bathed in 10 μM ATX II (*B* and *C*). The fibres in *B* and *C* both generated persistent trains of action potentials after 150 ms current injection.

10 μM. In every fibre for which the spike duration was unequivocally prolonged, repetitive firing was elicited by long-duration current injections. The converse was not always true. Some fibres exhibited repetitive firing without a significant increase in action potential duration (Fig. 6*B*).

Several features of the repetitive firing present in other models or diseases with myotonia were not produced by ATX II. Unlike muscle from the myotonic goat, muscle in chloride-free Ringer solution (Adrian & Bryant, 1974), or muscle from 20,25-diazocholesterol-fed rats (Furman & Barchi, 1981), there was no decrease in the total membrane conductance in the vicinity of the resting potential. The input resistance computed from the electronic responses in control and toxin-treated muscle was not significantly different (303 and 326 kΩ, respectively). The changes in action potential generation that accompany a decrease in resting conductance were also not present in the ATX II-treated fibres. In particular, there was no reduction in the threshold current for firing, and the latency to fire at threshold was not increased.

Evidence for multiple stable resting potentials

Because ATX II does not shift the voltage dependence of activation in sodium channels (Bergman *et al.* 1976), and the vast majority of channels are closed at

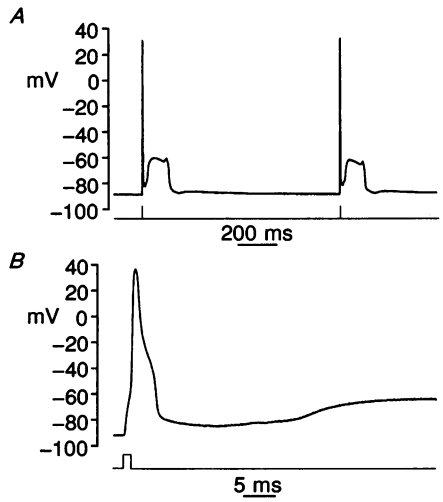

Fig. 7. Plateau depolarizations demonstrate a metastable resting potential in ATX II exposed fibres. *A*, action potentials elicited by 1·5 ms current pulses presented once every second. After each spike the resting potential shifts transiently to −60 mV. The same response is reproduced in *B* on a faster sweep speed.

potentials negative to −60 mV, the resting potential would not be expected to change spontaneously in ATX II-treated fibres. The resting potential measured by the initial impalement with a microelectrode was not significantly changed by low concentrations of toxin, and was mildly depolarized in 10 μM ATX II (−58 mV, compared to −69 mV in control fibres). With stimulation of toxin-exposed fibres, however, many sodium channels open and some may remain in a conducting state. This persistent inward current causes an inflection in the steady-state current–voltage relationship and creates the possibility of a second, metastable equilibrium potential at which the net transmembrane current is zero (see Fig. 9). The prediction is that a second stable resting potential may exist at a more depolarized potential.

Depolarized plateau potentials often occurred transiently after current injection in ATX II-treated fibres. Figure 5*D* shows a steady depolarized shift to −32 mV after a train of spikes. These plateau potentials persisted from several seconds to a minute or more, after which the prestimulus resting potential was re-established. On rare occasions a brief stimulus, which induced only a single action potential, caused a transient depolarizing shift. Figure 7 shows a 30 mV depolarization to a metastable resting potential following a single spike. Depolarizing shifts did not occur in control fibres. In addition, the magnitude of the depolarization far exceeded the shift expected from a T-tubular accumulation of potassium following a single discharge. Thus the plateau depolarizations in ATX II-treated fibres may represent a second, metastable resting potential.

Detubulation with glycerol prevents repetitive firing after the stimulus

A repetitive train of action potentials in muscle causes a depolarizing after-potential of about 1 mV per impulse which then decays with a half-time of approximately 0·5 s. Freygang, Goldstein & Hellam (1964) proposed that potassium accumulation in an 'intermediary space', now known to be the T-tubule system,

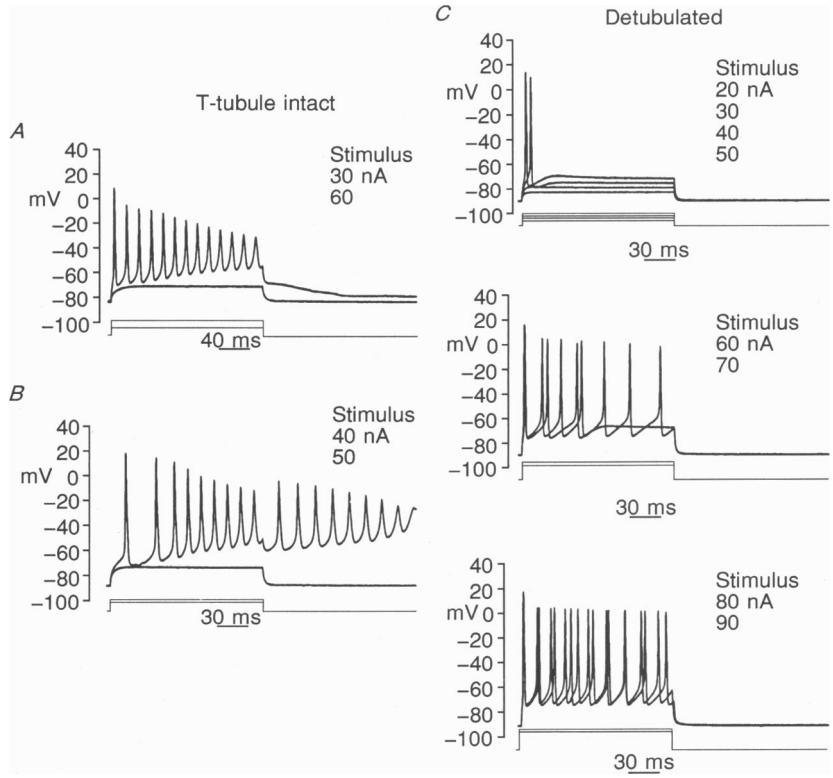

Fig. 8. The T-tubular system is necessary for depolarizing shifts during repetitive spikes and for after-discharges in ATX II-treated fibres. Fibres with intact T-tubule systems (*A* and *B*) show a progressive depolarizing shift in transmembrane potential at the end of each stimulus-induced spike. This shift generated either a persistent after-depolarization or runs of post-stimulus discharges. The detubulated fibre (*C*) never produced depolarizing shifts, after-depolarizations, or post-stimulus discharges, even with current intensities exceeding twice threshold.

causes the depolarization. Glycerol treatment was effective in electrically decoupling the surface and T-tubule membranes as demonstrated by a decrease in capacitance from 5·9 to 2·0 μF/cm^2. Figure 8 shows the effect of decoupling on the after-depolarization and repetitive spikes in ATX II-treated fibres. Intact fibres (Fig. 8*A* and *B*) had depolarizing shifts in transmembrane potential at the end of each spike and prominent after-depolarizations. The depolarizing shift did not occur with subthreshold current intensities, even with prolonged stimulus durations. In addition, the after-depolarization elicited by repetitive spikes decayed much more slowly than the relaxation at the end of a subthreshold current

injection. Occasionally, the after-depolarization elicited a train of discharges after the termination of the stimulus (Fig. 8*B*). In detubulated, ATX II-treated fibres, repetitive discharges did occur during the current injection, but after-spikes were never observed. Detubulated fibres (Fig. 8*C*) never produced after-depolarizations following a train of spikes. Thus we conclude that the actions of ATX II on sodium channels create the possibility for the repetitive discharges in muscle, but that an additional depolarizing influence, dependent on the integrity of the T-tubule system, is required to produce the post-stimulus firing characteristics of myotonia.

DISCUSSION

A small proportion of non-inactivating sodium channels is sufficient to cause myotonia

The principal finding of this study is the demonstration that both the electrical and the mechanical features of myotonia can be produced by a failure of inactivation in a relatively small proportion of sodium channels. Although it has been previously established that ATX II slows the relaxation of the twitch response (Alsen *et al.* 1981), induces a hyperexcitable state with trains of repetitive action potentials (Erxleben & Rathmayer, 1984; Harris *et al.* 1985), and disrupts the inactivation of sodium channels in patch-clamp recordings (Nagy, 1988), no previous investigations examined all these effects simultaneously. We now provide quantitative results that allow a correlation to be made between the extent of the alteration in sodium channel gating and the appearance of myotonia. It is important to define this correlation because two independent studies have proposed that hyperkalaemic periodic paralysis, and possibly other myotonic disorders, are caused by the failure of a small proportion of mutant sodium channels to inactivate normally (Cannon *et al.* 1991; Lehmann-Horn *et al.* 1991).

In confirmation of previous studies (Nagy, 1988), we found that the primary effect of ATX II on sodium channels is an alteration in the kinetics of inactivation. The proportion of sodium channels that display abnormal gating during a single depolarizing voltage step, however, was relatively small for micromolar amounts of ATX II. For patches containing two to four sodium channels, typically only one channel gated in the non-inactivating mode, and did so in a cluster of five to ten sweeps out of 100 trials. In 10 μM ATX II the time-averaged open probability, $< P_{open} >$, was 0·018 over the interval from 5 to 40 ms. This degree of aberrant gating is comparable, quantitatively, to the K^+-induced alteration in sodium channel behaviour that we measured in myotubes cultured from a patient with hyperkalaemic periodic paralysis (Cannon *et al.* 1991). In the HPP study, the sodium channel abnormality was quantified as the fraction of trials for which a mutant channel gated in the non-inactivating mode, and was determined to be 0·04–0·10. Since the steady-state open probability while in the non-inactivating mode was 0·5, then the equivalent $< P_{open} >$ for HPP muscle in 10 mM K^+ was 0·02–0·05.

The present study confirms that the small $< P_{open} >$ that we measured for HPP myotubes in culture should have a profound effect on the function of skeletal muscle. The development of myotonia in the rat EDL was steeply dependent on concentration, with an abrupt onset between 5 and 10 μM ATX II (cf. Fig. 4). In this range of toxin concentration $< P_{open} >$ was only 0·015–0·02, yet this was

sufficient to cause trains of discharges persisting beyond the duration of the stimulus to appear regularly. The after-discharges and prolonged relaxation were myotonic in origin, as opposed to neurogenic, because all bath solutions contained *d*-tubocurare. Many previous studies have focused on the increased duration of the action potential produced by ATX II (Alsen *et al.* 1981; Erxleben & Rathmayer, 1984; Harris *et al.* 1985; Kahn, Lemeignan & Molgo, 1986). At low concentrations of toxin, the action potential duration was often indistinguishable from controls (cf. Fig. 6), and yet a sufficient proportion of sodium channels was affected to cause repetitive discharges during long injections of current. Thus, the response to prolonged current injection is a more sensitive index of altered excitability than the duration of the action potential. With 10 μM ATX II, we observed a 2- to 3-fold increase in the spike duration. Fibres with widened action potentials always discharged in repetitive trains that often outlasted the stimulus.

In HPP, an initial myotonia progresses to paralysis. Although we were not able to produce paralysis in our toxin model, it has been induced by ATX II in the rat hemidiaphragm (Alsen *et al.* 1981) and the frog semitendinosus (Khan *et al.* 1986), with higher concentrations, longer exposure times, or increased toxin potency. Both species and fibre type differences may account for variations in potency among various preparations (Harris *et al.* 1985). We have, however, shown by computer simulation that only a small additional increase in $< P_{open} >$ is required to produce paralysis (Cannon, Brown & Corey, 1993). When $< P_{open} >$ was set to 0·025–0·05, then the membrane potential settled to a depolarized value after an action potential similar to that of the response in Fig. 7. From this depolarized resting potential the model (or a fibre) was refractory to discharging in response to any further stimuli and thereby produced paralysis. The model also demonstrated that the generation of repetitive after-discharges that persist during myotonia depends on a T-tubule compartment in which K^+ can accumulate.

To summarize, we envisage a spectrum of effects on membrane excitability caused by incomplete inactivation of sodium channels. Below 0·05–0·1 μM ATX II, $< P_{open} >$ is less than 0·001, and the response to either brief or long current steps is normal. In the range of 0·1– 5 μM, repetitive discharges occur during long steps of current injection, but after-discharges are absent, twitch relaxation is normal, and the duration of discharges elicited by brief injections is normal. $< P_{open} >$ would be about 0·01. With 5–20 μM ATX II, trains of action potentials continue beyond the duration of the current injection as after-discharges, the action potential is unequivocally widened, myotonia occurs, and $< P_{open} >$ is approximately 0·02. When $< P_{open} >$ exceeds about 0·04, then flaccid paralysis occurs.

Comparison to myotonia associated with a low chloride conductance

A reduction in the chloride conductance, g_{Cl}, of the sarcolemmal membrane is the major abnormality found in the myotonic goat (Bryant, 1962), myotonia congenita in man (Lipicky *et al.* 1971), and a recessive myotonia in mice (Mehrke *et al.* 1988). The electromyogram shows the same primary abnormality – runs of myotonic discharges – in all these disorders as well as in two diseases thought to be caused by sodium channel defects: paramyotonia congenita and hyperkalaemic periodic

paralysis. There are several important differences, however, between the electrical behaviour of myotonic muscle with low g_{Cl} and that of myotonic muscle with non-inactivating sodium channels. With low g_{Cl}, the total membrane conductance is dramatically reduced, while with non-inactivating sodium channels it is normal in

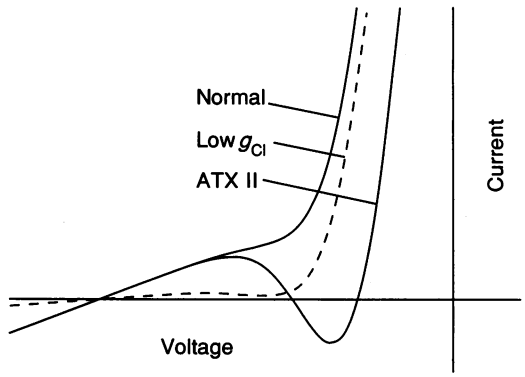

Fig. 9. Qualitative model of the current–voltage relationship at steady state. Heavy line depicts the prediction for normal muscle. Dashed line represents the low g_{Cl} condition, and the light line shows the response with a small proportion of non-inactivating sodium channels. See text for details.

the region of the resting potential. The threshold current intensity to elicit an action potential is markedly reduced and the latency to discharge is increased in the low g_{Cl} condition (Adrian & Bryant, 1974), but both are unchanged by the HPP–ATX II defect.

The current–voltage relationship has a reduced slope in the low g_{Cl} condition, but has a new inflection when sodium channels fail to inactivate. Qualitative current–voltage relationships are shown in Fig. 9 for normal muscle, low-g_{Cl} fibres, and cells with a small proportion of non-inactivating sodium channels. It represents a highly simplified model containing only a leak (chloride) conductance, an outwardly rectifying potassium conductance, and a sodium conductance that is normally inactivated at the steady state. The curve for normal muscle is dominated by g_{Cl} near the resting potential and then exhibits a large increase in conductance for depolarized potentials because of the outwardly rectifying K^+ current. The low-g_{Cl} case has a reduced slope in the vicinity of the resting potential, which leads to the instabilities and repetitive firing in a complete dynamic model of myotonic muscle. Note, however, that there is no change in resting potential at the steady state. The non-inactivating sodium channels allow a large, persistent inward current to develop for small depolarizations from the normal resting potential. This creates the inflection in the current–voltage relationship and causes the curve to cross the abscissa three times instead of once. The extreme leftward and rightward zero crossings are possible resting potentials while the middle one is always unstable. Thus in HPP or in ATX II-exposed muscle there could be a second possible stable equilibrium potential, depolarized relative to normal. This second resting potential is manifest as the plateau depolarization in Fig. 7 and the steady

depolarization frequently observed following the trains of after-discharges (cf. Figs 5*D* and 8*B*). Excessively depolarized fibres are commonly observed during a paralytic attack in HPP, but do not occur in pure forms of myotonia without weakness such as myotonia congenita.

There is one important similarity between the myotonia in muscle with low g_{Cl} and in fibres with non-inactivating sodium channels. In both conditions, the persistence of repetitive discharges beyond the duration of the current injection requires the integrity of the T-tubule system. Adrian & Bryant (1974) showed in goat muscle with a low g_{Cl} that both the after-depolarization and the repetitive discharge that follow long-duration current injections are abolished by detubulation with glycerol treatment. They proposed that the train of discharges is driven by a cumulative after-depolarization, which in turn arises from potassium accumulation in the T-tubule. As in the low-g_{Cl} condition, ATX II-exposed fibres also developed a cumulative depolarization during repetitive firing, an after-depolarization, and train of after-discharges. Furthermore, all these effects were absent in detubulated fibres (cf. Fig. 8). Thus both the low chloride conductance and the non-inactivating sodium channels create a hyperexcitable state in the muscle membrane with the potential for myotonic discharges, but an additional depolarizing influence from potassium-laden T-tubules is required to drive the repetitive firing.

Single channel studies in sarcolemmal spheres

Mechanically disrupted blebs or spheres of sarcolemmal membrane have been used in several studies to measure unitary currents from a variety of channels (Stein & Palade, 1989). The technique is relatively simple, fast, and free of potential complicating effects from enzymatic degradations used in chemical dissociations of tissue. The spheres were sufficiently free of debris to allow high-resistance seals to form with the patch electrode. In our hands, however, the technique was limited to the cell-attached and excised inside-out modes of recording because the mechanical fragility of the spheres did not permit 'whole-bleb' recording. The range of holding potentials and depolarized steps required to elicit sodium channel openings both imply that the resting potential of the membrane spheres was near 0 mV.

The bleb technique is well suited for measuring sodium channel behaviour in small fragments of muscle such as those obtained from open biopsies. Therefore, it is important to establish that mechanical disruption of the sarcolemma does not modify the gating of sodium channels. In other preparations, physical manipulation of the membrane has been associated with an alteration in gating. Kirsch & Brown (1989) have demonstrated that patch excision from the cell-attached to inside-out recording modes induces a partial loss of inactivation in sodium channels of cardiac myocytes. In our toxin-free bleb-attached patches, the probability of openings late in the depolarization was not significantly higher than that reported in other preparations. In patches on amphibian skeletal muscle that contained several hundred channels, Patlak & Ortiz (1986) occasionally observed repetitive bursting of a single non-inactivating sodium channel late in the depolarization. The amplitude of the persistent current was 0·12 % of the peak

early current at a test potential of −20 mV. The steady-state open probability was 0·11 % in our control patches. Since the peak in the open probability for a single channel was 0·4 at −20 mV (cf. Fig. 1), the ratio of peak to steady-state current was 0·28 %. Thus, within a factor of two, the extent of non-inactivation measured in the mechanically disrupted blebs was not different from other measurements of gating for the skeletal muscle sodium channel.

The authors wish to thank W. A. Catterall for suggesting the use of ATX II to mimic the loss of sodium channel inactivation observed in HPP muscle. This work was supported by a fellowship from the Charles A. Dana Foundation (S.C.C.) and by the Howard Hughes Medical Institute (S.C.C. and D.P.C.).

REFERENCES

ADRIAN, R. H. & BRYANT, S. H. (1974). On the repetitive discharge in myotonic muscle fibres. *Journal of Physiology* **240**, 505–515.

ALSEN, C., HARRIS, J. B. & TESSERAUX, I. (1981). Mechanical and electrophysiological effects of sea anemone (*Anemonia sulcata*) toxins on rat innervated and denervated skeletal muscle. *British Journal of Pharmacology* **74**, 61–71.

BERGMAN, C., DUBOIS, J. M., ROJAS, E. & RATHMAYER, W. (1976). Decreased rate of sodium channel conductance inactivation in the node of Ranvier induced by a polypeptide toxin form sea anemone. *Biochimica et Biophysica Acta* **455**, 173–184.

BRYANT, S. H. (1962). Muscle membrane of normal and myotonic goats in normal and low external chloride. *Federation Proceedings* **21**, 312.

CANNON, S. C., BROWN, R. H. & COREY, D. P. (1991). A sodium channel defect in hyperkalemic periodic paralysis: potassium-induced failure of inactivation. *Neuron* **6**, 619–626.

CANNON, S. C., BROWN, R.H. & COREY, D. P. (1993). Theoretical reconstruction of myotonia and paralysis caused by incomplete inactivation of sodium channels. *Biophysical Journal* (in the Press).

CANNON, S.C. & STRITTMATTER, S.M. (1993). Functional expression of sodium channel mutations identified in families with periodic paralysis. *Neuron* **10**, 317–326.

DULHUNTY, A. F. & GAGE, P. W. (1973). Differential effects of glycerol treatment on membrane capacity and excitation–contraction coupling in toad sartorius fibres. *Journal of Physiology* **234**, 373–408.

EBERS, G. C., GEORGE, A. L., BARCHI, R. L., TING-PASSADOR, S. S., KALLEN, R. G., LATHROP, G. M., BECKMANN, J. S., HAHN, A. F., BROWN, W. F., CAMPBELL, R. D. & HUDSON, A. J. (1991). Paramyotonia congenita and hyperkalemic periodic paralysis are linked to the adult muscle sodium channel gene. *Annals of Neurology* **30**, 810–816.

ELLIS, K. O. & BRYANT, S. H. (1972). Excitation–contraction uncoupling in skeletal muscle by Dantrolene sodium. *Naunyn-Schmiedeberg's Archives of Pharmacology* **274**, 107–109.

ERXLEBEN, C. & RATHMAYER, W. (1984). Effects of the sea anemone *Anemonia sulcata* toxin II on skeletal muscle and on neuromuscular transmission. *Toxicon* **22**, 387–399.

FONTAINE, B., KHURANA, T. S., HOFFMAN, E. P., BRUNS, G. A. P., HAINES, J. L., TROFATTER, J.A., HANSON, M. P., RICH, J., MCFARLANE, H., MCKENNA, Y. D., ROMANO, D., GUSELLA, J. F. & BROWN, R. H. JR (1990). Hyperkalemic periodic paralysis and the adult muscle sodium channel α-subunit gene. *Science* **250**, 1000–1002.

FREYGANG, W. H., GOLDSTEIN, D. A. & HELLAM, D. C. (1964). The after-potential that follows trains of impulses in frog muscle fibres. *Journal of General Physiology* **47**, 929–952.

FURMAN, R. E. & BARCHI, R. L. (1981). 20,25-Diazocholesterol myotonia: an electrophysiological study. *Annals of Neurology* **10**, 251–260.

HARRIS, J. B., POLLARD, S. & TESSERAUX, I. (1985). The effects of *Anemonia sulcata* toxin II on vertebrate skeletal muscle. *British Journal of Pharmacology* **86**, 275–286.

KHAN A. R., LEMEIGNAN, M. & MOLGO, J. (1986). Effects of toxin II from the sea anemone *Anemonia sulcata* on contractile and electrical responses of frog skeletal muscle fibres. *Toxicon* **24**, 373–384.

KIRSCH, G. E. & BROWN, A. M. (1989). Kinetic properties of single sodium channels in rat heart and brain. *Journal of General Physiology* **93**, 85–99.

KOCH, M. C., STEINMEYER, K., LORENZ, C., RICKER, K., WOLF, F., OTTO, M., ZOLL, B., LEHMANN-HORN, F., GRZESCHIK, K. & JENTSCH, T. J. (1992). The skeletal muscle chloride channel in dominant and recessive human myotonia. *Science* **257**, 797–800.

LEHMANN-HORN, F., IAIZZO, P. A., HATT, H. & FRANKE, C. (1991). Altered gating and conductance of Na channels in hyperkalemic periodic paralysis. *Pflügers Archiv* **481**, 297–299.

LEHMANN-HORN, F., KÜTHER, G., RICKER, K., GRAFE, P., BALLANYI, K. & RÜDEL, R. (1987). Adynamia episodica hereditaria with myotonia: a non-inactivating sodium current and the effect of extracellular pH. *Muscle and Nerve* **10**, 363–374.

LEIBOWITZ, M. D., SUTRO, J. B. & HILLE, B. (1986). Voltage-dependent gating of veratridine-modified Na channels. *Journal of General Physiology* **87**, 25–46.

LIPICKY, R. J., BRYANT, S. H. & SALMON, J. H. (1971). Cable parameters, sodium, potassium and chloride and water content and potassium efflux in isolated external intercostal muscle of normal volunteers and patients with myotonia congenita. *Journal of Clinical Investigation* **50**, 2091–2103.

MCCLATCHEY, A. I., VAN DEN BERGH, P., PERICAK-VANCE, M. A., RASKIND, W., VERELLEN, C., MCKENNA-YASEK, D., RAO, K., HAINES, J. L., BIRD, T., BROWN, R. H. & GUSELLA, J. F. (1992). Temperature-sensitive mutations in the III–IV cytoplasmic loop region of the skeletal muscle sodium channel gene in paramyotonia congenita. *Cell* **68**, 769–774.

MEHRKE, G., BRINKMEIR, H. & JOCKUSCH, H. (1988). The myotonic mouse mutant ADR: electrophysiology of the muscle fibre. *Muscle and Nerve* **11**, 440–446.

NAGY, K. (1988). Mechanism of inactivation of single sodium channels after modification by chloramine-T, sea anemone toxin and scorpion toxin. *Journal of Membrane Biology* **106**, 29–40.

PATLAK, J. D. & ORTIZ, M. (1986). Two modes of gating during late Na^+ channel currents in frog sartorius muscle. *Journal of General Physiology* **87**, 305–326.

PTACEK, L. J., GEORGE, A. L., GRIGGS, R. C., TAWIL, R., KALLEN, R. G., BARCHI, R. L., ROBERTSON, M. & LEPPERT, M. F. (1991 *a*). Identification of a mutation in the gene causing hyperkalemic periodic paralysis. *Cell* **67**, 1021–1027.

PTACEK, L. J., TRIMMER, J. S., AGNEW, W. S., ROBERTS, J. W., PETAJAN, J. H. & LEPPERT, M. (1991 *b*). Paramyotonia congenita and hyperkalemic periodic paralysis map to the same sodium-channel gene locus. *American Journal of Human Genetics* **49**, 851–854.

RICKER, K., CAMACHO, L. M., GRAFE, P., LEHMANN-HORN, F. & RÜDEL, R. (1989). Adynamia episodica hereditaria: what causes the weakness? *Muscle and Nerve* **12**, 883–891.

ROJAS, C. V., WANG, J., SCHWARTZ, L. S., HOFFMAN, E. P., POWELL, B. R. & BROWN, R. H. (1991). A Met-to-Val mutation in the skeletal muscle Na channel α-subunit in hyperkalemic periodic paralysis. *Nature* **354**, 387–389.

RÜDEL, R. & LEHMANN-HORN, F. (1985). Membrane changes in cells from myotonia patients. *Physiological Reviews* **65**, 310–356.

STEIN, P. & PALADE, P. (1989). Patch clamp of sarcolemmal spheres from stretched skeletal muscle fibres. *American Journal of Physiology* **256**, C434–440.

STEINMEYER, K., KLOCKE, R., ORTLAND, C., GRONEMEIER, M., JOCKUSCH, H., GRÜNDER, S. & JENTSCH, T. (1991). Inactivation of muscle chloride channel by transposon insertion in myotonic mice. *Nature* **354**, 304–308.

ULBRICHT, W. (1969). The effect of veratridine on excitable membranes of nerve and muscle. *Ergebnisse der Physiologie* **61**, 18–71.